



Simultaneous temporal, spatial and size-resolved measurements of aerosol particles in closed indoor environments applying mobile filters in various use-cases

Julia Szabadi^{a,*}, Jörg Meyer^a, Martin Lehmann^b, Achim Dittler^a

^a Institute of Mechanical Process Engineering and Mechanics, Karlsruhe Institute of Technology, Germany

^b MANN+HUMMEL GmbH, Ludwigsburg, Germany

ARTICLE INFO

Keywords:

Mobile air filter
Indoor air quality
Aerosol particle dispersion
Reduction of aerosol concentration
Testing under realistic conditions
Particle measurement

ABSTRACT

This paper focuses on simultaneous, time- and space-resolved measurements of particle size distributions in three different closed indoor environments (small office room, elementary-school classroom, and seminar room) applying mobile air filters in four scenarios (decay curves, filtration while people are present, a temporal strong point source, impact of filter orientation & cross-flow ventilation). The experiments reveal, that mobile indoor air filters, equipped with high-performance filter media (HEPA - quality), remove particles in the investigated rooms in relevant submicron size classes ($x < 1 \mu\text{m}$) efficiently and uniformly over time.

For the description of the local decrease in particle concentration a simple mathematical model based on a transient continuous stirred tank reactor was applied. The local decay curves obtained in the different room-types were compared to simulated ones assuming ideal mixing of the indoor air. The real-room scenarios show a slower particle decay than the predicted ones assuming ideal mixing of the indoor air. The experiments reported in this contribution demonstrate, that indoor air filters, operated with a filtration rate of 3.5 h^{-1} and positioned correctly, are capable of lowering the particle concentration in all relevant size classes in real-world closed indoor environments slowly over time (e.g. a reduction in particle concentration of 50 % after 30 min in a classroom w/o particle sources). In the investigated set-ups, at filtration rates above 9 h^{-1} , the filters' performance is close to cross-flow window-ventilation. The experiments reveal, that mobile air filters cannot avoid close distance transmission of submicron aerosol particles from one person to another. Therefore, they do not replace any of the well-known methods to avoid aerosol-driven infection (like wearing an efficient face mask correctly, limiting the number of people and time of stay in closed indoor environments, frequent ventilation). Mobile air filter devices may represent an additional component in an entire prevention strategy, especially when rooms cannot be ventilated regularly, efficiently or the constellation of people in groups changes frequently (e.g. waiting areas).

1. Introduction

Airborne aerosol particles are released continuously by breathing, speaking, singing, shouting, coughing, or sneezing and are

* Corresponding author.

E-mail address: julia.szabadi@kit.edu (J. Szabadi).

consequently dispersed in the surrounding air. Aerosol particles are considered the main transmission path of the SARS-CoV2 (Jayaweera et al., 2020; Kähler & Hain, 2020; Lu et al., 2020; Morawska & Cao, 2020; Zhang et al., 2020). Many studies show that exhaled aerosol particles, in particular, play a crucial role in the indoor spread of viruses, where the risk of infection is increased (Fabian et al., 2008; Lindsley et al., 2016; Milton et al., 2013; Morawska & Cao, 2020). The size of exhaled aerosol particles is typically $x < 1 \mu\text{m}$ (Haslbeck et al., 2010; Schwarz et al., 2010, 2015). Aerosol particles generated by speaking and singing have a size of about $x = 1 \mu\text{m}$ (Asadi et al., 2019). The concentration of exhaled virus-laden particles in a room depends on the number of (infectious) persons present, the length of their stay in the room, their activity and age. A healthy person exhales between one and a few hundred aerosol particles per liter of air during respiration without exhausting physical activity (GAeF, 2020; Hartmann et al., 2020). According to Scheuch (Scheuch, 2020), exhaled particles are within a size range of $x = 0.1\text{--}0.5 \mu\text{m}$, while other studies classify them in a tighter size range of $x = 0.15\text{--}0.2 \mu\text{m}$ (Edwards et al., 2004). In many studies, the lower measurement limit for exhaled aerosol particles is often $x = 0.3$ or $0.5 \mu\text{m}$ due to metrological restrictions, resulting in lower particle number (PN) concentrations for the exhaled particulate aerosols (GAeF, 2020).

Particle dispersion in closed rooms may be influenced by size-dependent particle transport and deposition phenomena. For example, a particle with an aerodynamic diameter of $x = 1 \mu\text{m}$ and the density of water would take about 7.5 h to sink to the ground from a height of 1 m, assuming a constant diameter during sedimentation (GAeF, 2020). Note that exhaled droplets evaporate in the air over time. Consequently, the size of the relevant aerosol particles dispersed in the ambient air can be much smaller than the size of the originally exhaled aerosol particles. Due to the small size $< 1 \mu\text{m}$, the sedimentation is hardly relevant for their deposition. The aerosol particles are rather transported with the airflow (GAeF, 2020) and their concentration can be reduced e.g. by ventilation systems or mobile air filters. In commercial indoor air filters, H13/H14 filter elements are often used for filtration to enable high separation efficiency of submicron particles, and thus, high particle removal rates. Similar removal rates can be achieved applying operational concepts with lower efficiency filters and compensating higher volume flow rates (ASHRAE, 2021), resulting in equivalent concentration reductions in the room.

There are several well-known ways to lower the concentration of aerosol particles or protect people from exposure to potentially contagious aerosols indoors. Besides wearing an efficient mask correctly, ventilation and the use of ventilation systems are widely discussed (GAeF, 2020). In addition, the application of mobile air filters to reduce particle load in closed indoor environments is proposed.

Mobile air filters draw the air through the filter medium and the particles are separated by different mechanisms like impaction, interception and diffusion, depending on their size.

Thus, during operation, they lower the PN concentration over time or keep it at a low level (Curtius et al., 2021; Kähler et al., 2020a; Küpper et al., 2019).

Many studies have shown which factors should be considered when selecting a mobile air filter, e.g. volume flow, noise level, or positioning of the device. With an increasing volume flow, the steady-state between the particle source and the particle sink (filter) is reached faster (Schumacher et al., 2021). However, the noise level of the blower increases with an increasing volume flow. Therefore the noise level during continuous operation and sufficiently high volume flow rates should be considered when selecting a device (Bluyssen et al., 2021). Multiple mobile air filters can also be placed in the room to enable a high volume flow and a relatively low noise level (Curtius et al., 2021).

In addition to the set volume flow, the temporal decrease in particle concentration through filtration may also be influenced by the location of installation and the geometry of the room (Kähler et al., 2020b). There are different conclusions in literature as to which extend the location of the device and possibly shielding objects influence the results of the filtering. While in some studies, the position and other objects in the room influence the particle reduction (Kähler et al., 2020a; Küpper et al., 2019; Narayanan & Yang, 2021; Novoselac & Siegel, 2009), others discover no influence of the positioning (Kähler et al., 2021; Küpper et al., 2019). According to Kähler et al. tables, chairs, computers or transparent protective walls have no negative effect on filter performance (Kähler et al., 2021). In elongated rooms, particles can be separated less efficiently, because a recirculation area is formed due to flow separation (Etheridge & Sandberg, 1996). In rooms with such geometries, several mobile air filters can be installed (Kähler et al., 2020b). In the listed studies (Kähler et al., 2020a, 2020b, 2021; Küpper et al., 2019; Narayanan & Yang, 2021; Novoselac & Siegel, 2009), the position of the mobile air filters' air outlets differs among the devices (outlet to the ceiling or to the side). However, a clear influence on complete or only partial mixing of the room air could not be derived from this.

The impact of mobile air filter operation in closed indoor environments on the temporal development of PN concentration in specific rooms has already been investigated and reported in several studies (Curtius et al., 2021; Kähler et al., 2020; Kähler et al., 2020b; Kähler et al., 2021; Küpper et al., 2019). Simultaneous measurements of the particle concentration at several room positions while applying different set-ups of mobile air filters have been reported (Kähler et al., 2020a, 2020b). However, the simultaneous temporal evolution of the local particle size distribution in different areas in real-world closed indoor environments has hardly been investigated and reported so far.

In this study, the evaluation of highly effective filters concerning the temporal-spatial evolution of particle size distribution and concentration is investigated for two mobile air filter devices in different operation modes. Four different scenarios (decay curves, filtration while people are present, a temporal strong point source, impact of filter orientation & cross-flow ventilation) are investigated in three rooms of different geometry and application (small office room, elementary-school classroom, and seminar room). At various defined filtration rates, decay curves were determined and compared to decay curves obtained from an ideal CSTR (continuously stirred tank reactor) mathematical model. The experiments were performed according to real conditions with people present (e.g. during elementary school lessons). The influence of people on the temporal and spatial development of the particle distribution and concentration was examined. In addition, the correlation between PN concentration and CO_2 concentration was investigated during a

school lesson. A temporal presence of a “superspreader” was simulated by a strong local point source to study the effect of filter operation on the temporal and spatial evolution of particle size distribution and concentration. Finally, the influence of the orientation of the filter unit and thus the location of air intake and outlet, on the decay curve in an elongated room was investigated. Decay curves of filter operation and cross-ventilation were compared.

2. Material and methods

To determine the temporally-, spatially-, and size-resolved evolution of the particle concentrations in different closed indoor environments, particles were generated representing the size distribution of exhaled particle residues. Measurements of the time-, and size-resolved evolution of the PN concentration at up to three different spots in each room, were carried out with three identical optical particle counters.

2.1. Aerosol generation

Sources of aerosols in everyday school classes may be e.g. speaking or breathing persons (students, teachers). The particle size that is generally produced by normal breathing and that is particularly common in the ambient air ranges between $x = 0.1\text{--}0.5\ \mu\text{m}$ (Scheuch, 2020). Based on this knowledge, particles with a number-weighted average particle diameter of $x = 0.113\ \mu\text{m}$ and a standard deviation of $0.127\ \mu\text{m}$ were generated in this study. In order to ensure a constant initial concentration level between the measurement series, an artificial aerosol source (AGK 2000 from Palas®) was used to generate a droplet aerosol from a sodium chloride (NaCl) solution (Table 1). The droplet aerosol is subsequently diluted with air, resulting in dry airborne NaCl particles.

Table 1
Technical data AGK 2000 (Palas®).

Technical data AGK 2000	
<i>Particles</i>	<i>Sodium chloride - particles</i>
<i>Average total PN concentration (at 0.8 bar at nozzle and 4 bar at dilution)</i>	<i>560,000 particles/cm³</i>
<i>x_{50,0} (measured by SMPS)</i>	<i>0.113 μm</i>
<i>Concentration of saline solution</i>	<i>16.6 % by weight</i>
<i>Total volume flow at the outlet</i>	<i>24.9 l/min</i>

2.2. Aerosol measurement technology

In order to detect the temporal evolution of size-resolved particle concentrations at different positions in each room, up to three optical particle counters (Fidas® Frog devices from Palas®) were used simultaneously. As specified by the manufacturer, the Fidas Frog detects particles in the size range of $x = 0.18\text{--}18\ \mu\text{m}$ and a concentration level of up to 20,000 particles/cm³. Table 2 gives all relevant technical specifications of the Fidas Frog. The measuring range of the Fidas Frog only covers the upper size range of the dry NaCl particles generated by the AGK 2000. Relevant concentration levels can still be measured in these size classes.

Table 2
Technical data Fidas® Frog (Palas®).

Technical data Fidas® Frog	
<i>Height x width x depth</i>	<i>100 mm × 240 mm x 150 mm</i>
<i>Measuring range</i>	<i>0.18 – 18 μm</i>
<i>Size channels</i>	<i>32/decade, 256 raw data channels</i>
<i>Measuring principle</i>	<i>Optical light scattering at the single particle</i>
<i>Measuring range (number CN)</i>	<i>0 – 20,000 particles/cm³</i>
<i>Sample flow</i>	<i>1.4 l/min</i>

3. Mobile air filters

Within the scope of this contribution, two different mobile air filters from MANN + HUMMEL were applied (OurAir TK 850 and OurAir SQ 2500). They differ in their volume flow range (Table 3) and the arrangement of the air intake and the air outlet. Regarding the TK 850, the air enters through holes at the bottom of the device, passes through a filter (Table 4), and discharges through perforated screens on the upper right and left of the side panels. In contrast, regarding the SQ 2500, the air is drawn in horizontally on the small side of the device and released at a 90° angle on the wide side of the unit. For simplification, the smaller TK 850 is called mobile air filter I, and the bigger SQ 2500 is called mobile air filter II. Other air purifiers described in literature are designed differently concerning the air intake and outlet orientation. Some blow filtered air upwards towards the ceiling, which could affect the flow pattern around the device and in the room. Therefore, the orientation of the device in the room needs to be considered.

The US-HEPA is used for the American market and the HEPA H14 for the European market.

Table 3
Technical Data of mobile air filter I and II (MANN+HUMMEL, 2020).

	Technical Data mobile air filter I	Technical Data mobile air filter II
Length x width x height	0.5 m × 0.55 m x 0.75 m	1.004 m × 0.523 m x 1.051 m
Weight	50 kg	170 kg
Flow rate	0 to 950 m ³ /h	0 to 2500 m ³ /h
Main Filter element	US HEPA, HEPA H14	HEPA H14
Prefilter	F7	F7
Figure of mobile air filter I and II (arrows indicate flow direction)		

Table 4
Technical Data of the filter elements (mobile air filter I).

Technical Data filter elements		
Filter element	US-HEPA	HEPA H14
Class	HYB5939 PerForm®	EN 1822 H14
Length x width x height	0.46 m × 0.46 m x 0.29 m	0.46 m × 0.46 m x 0.29 m
Filter face velocity	1.2 cm/s	2.3 cm/s
Weight	68 g/m ²	88 g/m ²
Filter area	20 m ²	10.4 m ²
Specified filter separation efficiency	≥ 99.97%	≥ 99.995%

3.1. Performance parameters: clean air delivery rate (CADR) and filtration rate

In order to compare the performance of mobile air filters considering the different room sizes, experimental conditions and settings (e.g. volume flow through the filter), a performance parameter is required. The CADR is the product of the flow rate and the filter efficiency and commonly applied for the evaluation of mobile air filters (including filter elements and flow rates). For marketing purposes, most manufacturers specify the maximum CADR, which is the performance parameter, where the air cleaner is operated at the highest possible flow rate. Consequently, this parameter represents the maximum possible performance of the mobile air filter.

However, according to e.g. GB/T 18,801:2015, the CADR is determined only locally at one point in a standardized (small) room volume, at the maximum volumetric flow rate and with permanent mixing of the indoor air. The CADR is derived from particle concentration decay curves, determined for different, defined test aerosols (pollen, fine dust, smoke). Therefore, the CADR only applies to the mentioned standard conditions and spatial geometries. In this study, the effectiveness of mobile air filters was investigated in realistic room setups with deviating room geometries and with a test aerosol, which differs from the specified ones in the standard. Thus, the filtration rate is defined to evaluate the performance of a mobile air filter in a given real environment. The filtration rate is specified as the ratio between the operating volume flow of the filter unit and the room volume. This results in the global decrease in concentration in the given space assuming perfect mixing and perfect filtering.

3.2. Mathematical model

In order to describe the local decrease in PN concentration, a simple mathematical model based on a transient continuous stirred-tank reactor (CSTR) was applied. The mathematical approach describes a monodisperse aerosol with the particle size x. The model

balances the time-dependent number of particles in the control volume $c_R(t)$. The control volume V_R is the volume of the room without filter. When the filter is in operation, particle-laden air with concentration c_R is removed from the room by the intake flow \dot{V}_F of the filter and the filtered identical volume flow is reintroduced into the room at the outlet of the filter with concentration c_{clean} (Fig. 1).

The particle number balance for a differential time step is then

$$\dot{V}_F (c_{clean} - c_R) dt = V_R \cdot dc_R \text{ with } c_{clean}(t) = P \cdot c_R(t)$$

The particle separation efficiency of the filter is described by the penetration P . Starting at the initial concentration c_0 at $t_0 = 0$, integration over time leads to the following equation

$$c_R(t) = c_0 \cdot \exp\left(-\frac{t}{\tau_F} (1 - P)\right) \text{ with } \tau_F = \frac{V_R}{\dot{V}_F}$$

The ratio of the room volume and the airflow rate corresponds to the global residence time τ_F and can be calculated from the operating conditions. For a highly efficient filter, the penetration approaches 0, resulting in the familiar mathematical description for a transient CSTR. The applied CSTR-based model assumes perfect mixing within the control volume. However, using τ_F is an approximation, which does not necessarily hold true for the experimental setups. The geometry of the room (aspect ratio, flow obstacles, etc.) and the size and orientation of the mobile air filter lead to a complex flow pattern in the control volume. As a result, some zones, mostly in large and elongated rooms, might experience a locally increased convective exchange of air, while other zones might show lower convective exchange rates (e.g. “dead zones” in corners far away from the filter). This deviation can be accounted for by using a local τ instead of the global τ_F for the perfectly mixed CSTR. This local τ can be derived from an approximation of the equation for $c_R(t)$ using a new coefficient τ_{exp} as a free parameter in a least squares (LS) approximation. A deviation of the local rate of particle removal can then be identified by comparing the τ_{exp} value to the nominal τ_F for ideal mixing conditions. Several additional modifications were made to the exponential fit function to account for further aspects of the experimental setup, which are not caught by the simple CSTR model:

A “dead time” term t_{dead} was added to account for a finite time needed for the transfer of cleaned airflow from the filter to the position of measurement and the startup of the blower inside the filter.

A base value for the particle concentration c_∞ after long-term operation of the filter was added to account for the effect of small leakages of outside air into the room introducing an additional steady non-negligible flux of particles to the control volume. c_0 then consists of $c_\infty + \Delta c_0$, and only Δc_0 is affected by the exponential decay over time. (Strictly speaking, the leakage would have to be taken into account by an additional term in the differential quantity balance, introducing additional unknown variables such as leakage rate and outside particle concentration. However, for small contributions, the leakage mainly affects the concentration values after a long time, while the short-term decay rate, and thus τ_{exp} , is almost unaffected). The initial concentration c_0 (for $t \geq t_{dead}$) was also derived from the LS-approximation rather than from averaging some initial concentration readings. This provides more reliable c_0 values and eliminates the uncertainties in determining the averaging interval – or, more precisely, the exact start of the concentration decay, which specifies the end of this interval.

Using the above modifications, the equation for $c(t)$ can be rewritten as

$$c(t) = \begin{cases} c_0 = \Delta c_0 + c_\infty & ; t \leq t_{dead} \\ \Delta c_0 \cdot \exp\left(-\frac{t - t_{dead}}{\tau_{exp}} \cdot (1 - P)\right) + c_\infty & ; t > t_{dead} \end{cases}$$

c_0 : initial PN concentration [particles/cm³]

c_∞ : PN concentration after infinite time of filter operation [particles/cm³]

Δc_0 : difference between c_0 and c_∞ [particles/cm³]

t : time [s]

t_{dead} : delay before the effect of the filter is noticed in the specific setup and room [s]

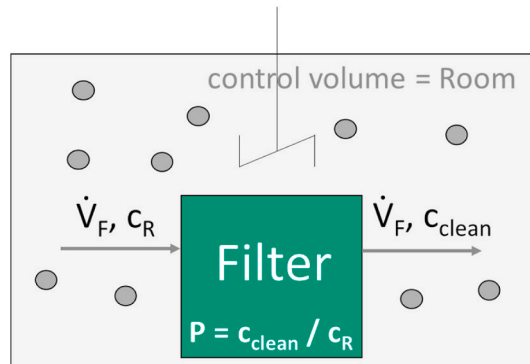


Fig. 1. CSTR with filter.

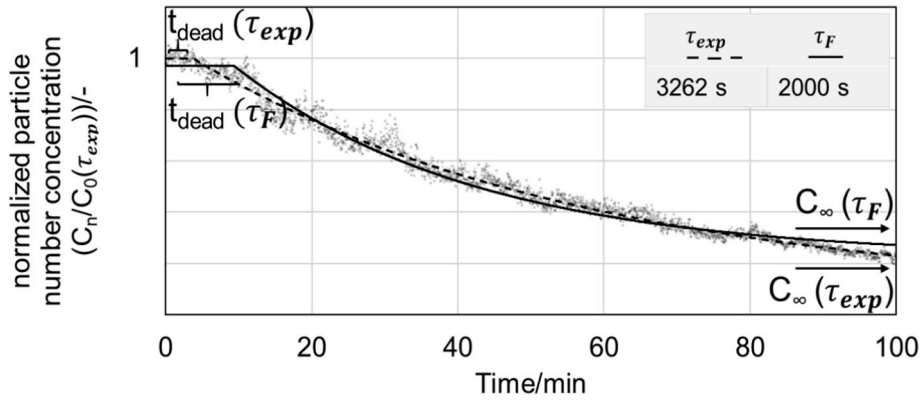


Fig. 2. Two variants of LS-approximations for a series of measurements of PN concentration (data compare to chapter II).

τ_{exp} : local residence time [s]

P: penetration of particles through the filter [–]

For all filter elements in this study, penetration was set to zero, which seems reasonable for the efficiency values given in Table 4. Even for the “lower” efficiency US-HEPA element, the resulting error in the τ_{exp} value is below 0.3 %. The LS-approximation was generally done using Δc_0 , c_∞ , t_{dead} and τ_{exp} as free fitting parameters (4-parameter “ τ_{exp} ” - fit). Fig. 2 shows the superiority (and thus, the necessity) of the 4-parameter fit over a 3-parameter fit with a fixed nominal global value τ_F (“ τ_F ”-fit).

The τ_{exp} -fit follows the experimental data very closely, while the τ_F -fit is less accurate, resulting in an overestimation of t_{dead} and c_∞ and an underestimation of c_0 . The clear superiority of the approximation using a local τ_{exp} instead of a nominal global τ_F indicates significant deviations of the local conditions for mixing and convective dilution from the average values.

In the example in Fig. 2, τ_{exp} is 63 % larger than τ_F , indicating significantly lower local flow rates of cleaned air compared to the average overall flow rate derived from the room volume and volume flow through the filter. A comparison of the two respective LS-approximations, based on the values for τ_F and τ_{exp} , will be used later in the interpretation of the experiments in different rooms and at different operational parameters of the filter. It allows distinguishing zones with high cleaning intensity from “dead zones” with lower concentration decay rates.

3.3. Overview of the test conditions

The effectiveness of two mobile air filters regarding the ability to lower the indoor particle concentration was examined in rooms of three different sizes (Table 5), similar to another study (Kähler et al., 2021). The main focus was to investigate the decrease in PN concentration depending on the filtration rate in different setups representing scenarios in real-world environments:

- **Scenario 1: “Decay curves”** (Filter operation without additional particle sources).
- **Scenario 2: “Filtration while people are present”** (Filter operation with people serving as an aerosol source within the room).
- **Scenario 3: “Temporal strong point source”** (Filter operation with an artificial particle generation in the room). The 3rd scenario represents the presence of an infected person in the room that exhales high amounts of contagious particles/droplets. Since the short-range effects of the point source are less affected by the entire volume of the room, the measurements were only carried out in the classroom.
- **Scenario 4: “Impact of filter orientation & cross-flow ventilation”** (Filter operation with different orientations of the mobile air filter.) Since the influence of short-circuit currents of the airflow is more noticeable in larger elongated rooms, this was investigated in the largest room, the seminar room, for two orientations of the mobile air filter.

Table 5 provides an overview of the four conducted scenarios and the particular test conditions in the three rooms.

Some of the scenarios were performed in all available rooms, while others focused on specific conditions that could only be studied selectively in a single room (e.g. scenario 4).

The different scenarios were realized with adapted (and thus different) experimental setups and measurement procedures. For scenario 1, the measurement data were approximated by an LS-approximation of a simple equation derived from a CSTR system (4-parameter fit). The effectiveness of the mobile air filters was tested in the rooms with various airflow rates (scenario 1). Starting with a small room (office) with few people as aerosol sources and a mobile air filter (I) set to the maximum specified flow rate of 950 m³/h, initial estimates of the PN concentration decay behavior were obtained. In the classroom to keep background noise low, the mobile air filter was only operated at approximately 80 % of its max. flow rate (770 m³/h). For comparison at a lower filtration rate with almost no ventilation noise, an additional flow rate of 400 m³/h was selected. A similarly large but more elongated-shaped room as the classroom with a more powerful mobile air filter (II) was used to test an even higher air flow rate. As in the office, the maximum volume flow was also selected to verify the maximum decrease in particle concentration.

Table 5
Overview of the scenarios and test conditions in the three application rooms.

Room	I Office	II Classroom	III Seminar room
\dot{V} (m^3/h)	950	400/770	2500
$V_{\text{Room}}/\text{m}^3$	103	222	268
Source	Persons	Aerosol generator/persons	Aerosol generator
Filter	US-HEPA	US-HEPA/HEPA H14	HEPA H14
Mobile air filter	I	I	II
Time-resolved	x	x	x
Spatially resolved		x	x
Size resolved		x	
CO_2		x	
Scenario			
1. Decay curves	x		x
2. Filtration while people are present		x	
3. Temporal strong point source		x	
4. Impact of filter orientation & cross-flow ventilation			x

By distributing the particle measuring devices in the rooms, the temporal and local development of the PN concentration and the particle size distribution in the rooms can be investigated. In all setups, no forced ventilation was employed (flow due to the mobile air filter only).

The four scenarios in the three use-cases (office, classroom, seminar room) are discussed below.

3.3.1. Application: office

The objective of the particle concentration measurements in the office was the validation of the LS-approximation via experimental data. Due to the comparably small room size of 103 m^3 , the measurement conditions are close to the assumptions made for the CSTR. Additionally, the maximum particle concentration decay was investigated (maximum flow rate & small room size).

3.3.1.1. Scenario 1: Decay curves. The evolution of the PN concentration was recorded at a single measurement point (F1). The mobile air filter I, equipped with the US-HEPA filter element, was positioned centrally on the longest wall of the room. Two experiments were performed. The room was ventilated for 15 min before each experiment to enable similar starting conditions, regarding particle concentration $c(t_0)$ for each run. After ventilating, the aerosol generator was operated for 60 min to generate a high initial particle concentration (higher than the ambient concentration) to measure the natural decrease in particle concentration without filtration, e. g. through diffusion or losses to the environment (natural convection through windows, doors). In the second experiment, three people serve as aerosol sources (talking, exhaling, etc.). After 60 min the “sources” left the room and the decrease in particle concentration at a flow rate of $\dot{V} = 950 \text{ m}^3/\text{h}$ was determined.

Fig. 3 shows the evolution of the normalized PN concentration in the office while the mobile air filter I is operated at a high filtration rate (close to ideal mixing) of 9.2 h^{-1} . Additionally, the natural concentration decrease without filter operation is illustrated.

In the case of ideal flow conditions, the average residence time in the office is $\tau_F = 390 \text{ s}$ ($\tau_F = 1/f$). Since the value of the actual required residence time τ_{exp} is larger than τ_F , the local mixing conditions appear to be worse than the global average. According to the mathematical model, for the defined conditions, the flow within the office appears to be not ideal. However, the experimental data show that at a high filtration rate of 9.2 h^{-1} , the PN concentration drops by 50 % after 5 min. No significant dead time occurred during the experiments in the small room. The long-term concentration c_∞ is low and is approximately $c = 2 \text{ particles}/\text{cm}^3$ for the calculated local residence time τ_{exp} .

3.3.2. Application: classroom

The objective of the classroom - experiments was the demonstration of three scenarios regarding the spatio-temporal particle concentration evolution and the change in (spatial) particle size distribution. Differences between the empty classroom (no people in the room), a typical school lesson (15 people in the room) and a simulated “superspreader” event (local temporal strong point source) were determined.

The range of the initial concentration resulted from the slightly different initial concentrations at the three measurement positions. The residence times τ_{exp} resulting from the LS- approximations for each position are summarized in the table of the figure. With a filtration rate of 1.8 h^{-1} (Fig. 4-left), in close proximity to the mobile air filter (F3), the particle concentration decreases slightly faster than at positions further away (F1, F2).

The spatial deviation of the temporal decrease in PN concentration is reflected in τ_{exp} . In case of ideal mixing, the concentration in all positions would decrease uniformly with a nominal residence time of $\tau_F = 2000 \text{ s}$ ($\tau_F = \frac{V_R}{V_F}$). Comparing the nominal residence time with the local residence time from the LS-approximation, the deviation increases with increasing distance from the mobile air filter. Thus, there seems to be local flow differences. In this study, no flow measurements were performed. Nonetheless, it is known from literature that airflow in a room is complex and influenced by many factors such as the geometry of the room, the velocity, the momentum at the supply terminal, the location of the supply and extract terminals or objects and furniture (Etheridge & Sandberg, 1996). If the flow dispersion is disturbed by, for example, an object, more complex indoor airflows are formed (Etheridge & Sandberg, 1996; Kähler et al., 2020a; Narayanan & Yang, 2021). These may lead to locally varying particle concentrations resulting in differences in residence time. However, as mentioned in the introduction, the influence of flow restriction like objects or a various positioning of the mobile air filter on the concentration decrease was evaluated differently by individual studies (Kähler et al., 2020a, 2020b, 2021; Küpper et al., 2019; Narayanan & Yang, 2021; Novoselac & Siegel, 2009). Therefore, further studies on this topic will be inevitable.

Comparing the different filtration rates, the concentration decreases faster at the higher filtration rate of 3.5 h^{-1} than at the lower filtration rate of 1.8 h^{-1} , which is similar to other investigations (Kähler et al., 2020a). In contrast to the measurements in the office, significant dead times are recorded in the range of up to 5 min at a filter rate of 1.8 h^{-1} in the classroom. An increase in filtration rate (3.5 h^{-1}) decreased the dead time to values below 3 min. At a filtration rate of 3.5 h^{-1} a reduction of the particle number concentration by 50 % is achieved after 20 min and at 1.8 h^{-1} after 50 min. The higher filtration rate seems to improve the flow conditions in the classroom in terms of more homogeneous mixing conditions at all measurement positions (F1–F3) since the local residence times differ by only a few seconds and the decay curves coincide. However, the decrease in PN concentration at the local measurement positions is significantly slower than expected from ideal CSTR behavior ($\tau_F = 1028 \text{ s}$). The deviation could possibly be explained by a “short-circuit flow” in the vicinity of the filter resulting in areas of lower volume flows for the remaining larger volume fraction of the room where all three instruments are positioned. Fig. 4 (right) shows the concentration curves of the two different filter elements at the identical filtration rate ($f = 3.5 \text{ h}^{-1}$). The concentration evolution of both measurements with the respective filter element is very similar.

Since only a nominal volume flow of an element is known, a deviation of the volume flows for different filter elements cannot be excluded. A lower filtration rate may slow down the decrease in particle concentration. However, the mean deviation at all three positions between the elements is rather small (max. 10 %). Accordingly, even with a filter element with a slightly lower filter efficiency (99.97 %), the concentration decreases at a similar rate as with an H14 filter element.

3.3.2.2. Scenario 2: filtration while people are present. In this scenario, the temporal, spatial, and additionally size-resolved development of the particle concentration was determined under real conditions (school lesson) to investigate the influence of people on the concentration decrease. The following measurement was carried out with a class of 13 students (without masks) and two adults (with masks) serving as aerosol sources. Two sets of experiments were performed. The first measurement examined the development of the particle concentration without filtering and the second with filtering. For the first experiment, the windows and doors were closed for

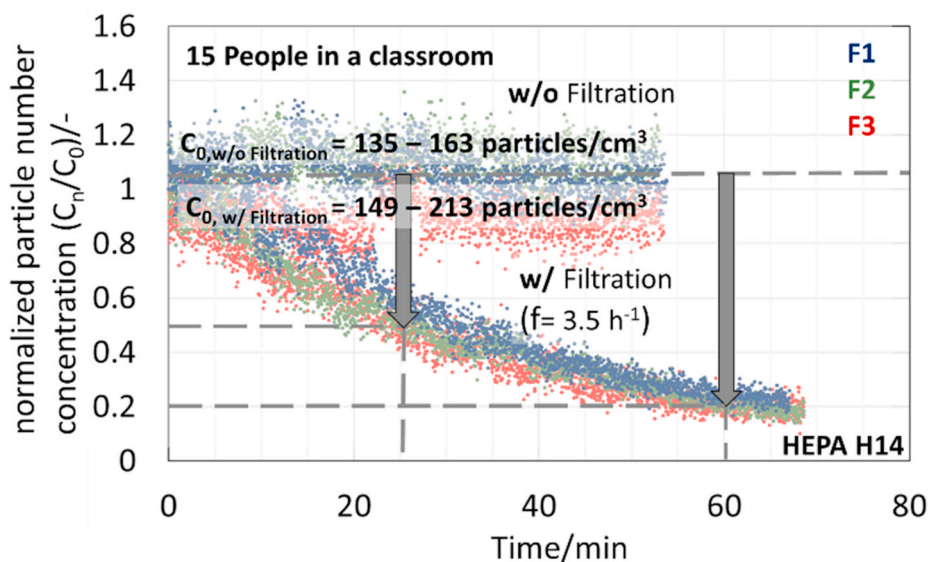


Fig. 5. PN concentration with and without filtration of indoor air – while people are present.

45 min after the initial ventilation phase (15 min) and the natural decrease in PN concentration was determined in the presence of the students in the room. For the second experiment, the classroom was ventilated again and the mobile air filter I ($\dot{V}= 770 \text{ m}^3/\text{h}$) was operated for 45 min during the school lesson. The deployed filter element was the HEPA filter H14. In addition to the PN concentration, the CO_2 concentration evolution was recorded by a hand-held instrument (CP11-Rotronic). The measurements should reveal if the CO_2 concentration correlates with the PN concentration.

Fig. 5 illustrates the local and temporal decrease in PN concentration with and without filtration at the three measurement positions F1–F3.

Without filtration, the initial concentration is $c = 135\text{--}163 \text{ particles}/\text{cm}^3$, depending on the position, and remains relatively constant over 50 min. The initial concentration corresponds to the concentration after ventilation (ambient conditions). Since the PN concentration does not increase noticeably due to the presence of people without filter operation, the majority of particles in the room may be attributed to the contribution of the outside aerosol (Chapter II scenario 1). In the case of the experiment including filter operation, the initial concentration is in a similar range of $c = 149\text{--}213 \text{ particles}/\text{cm}^3$. Filtration lowers the PN concentration despite the constant presence of aerosol sources (people in the room). After 25 min, half of the particles are removed from the indoor air, and after 60 min a reduction of 80 % is achieved. In scenario 1 (without people in the room) the concentration drops slightly faster. A reduction of 50 % is achieved after 20 min and of 80 % after 50 min (compare Fig. 4-right). The study by Hartmann has shown that healthy people only produce a few particles per liter (Hartmann et al., 2020). Accordingly, the slightly slower decrease in particle concentration cannot be explained by the contribution of exhaled particles.

Fig. 6 displays the particle size distributions during the two measurement series at the beginning and end of the respective experiment (compare Fig. 5) of all the three local measurement positions (F1 – F3). On the left, the entire detectable size range of the Fidas® Frog is shown. For improved visibility, a detailed view of the size range of $x = 1\text{--}20 \mu\text{m}$ has been added on the right side of Fig. 6. The particle size distributions depict that the majority of particles are present in the size classes ranging from $x = 0.2\text{--}0.3 \mu\text{m}$. Other studies have already shown that the particle sizes of exhaled aerosols are mainly in this size range (Schwarz, 2012). Nonetheless, measurement limitations of optical detection towards smaller particles have to be taken into account. In the measurement series without filtration, the total number of particles increases slightly within 50 min of the experiment in the size classes of $x = 0.2\text{--}0.3 \mu\text{m}$ from a maximum of $c = 26 \text{ particles}/\text{cm}^3$ up to $c = 37 \text{ particles}/\text{cm}^3$.

In the experiment with filter operation, the number of particles in the size classes of $x = 0.2\text{--}0.3 \mu\text{m}$ decreases significantly from a maximum of $c = 41 \text{ particles}/\text{cm}^3$ down to $c = 7.5 \text{ particles}/\text{cm}^3$ within 50 min. This corresponds to a separation of potentially infectious aerosols of approximately 82 %. The PN concentration of fractions $x > 1 \mu\text{m}$ is very low in both experiments (with and without filtering indoor air) and fluctuates by less than $1 \text{ particle}/\text{cm}^3$. Due to the temporary activity of the students in the room (walking around), the number of particles in the size classes $x > 1 \mu\text{m}$ increases slightly compared to the start (t_0) of the measurement. However, the number of particles in the size classes $x > 1 \mu\text{m}$ ($t = 50 \text{ s}$) is lower using filters than without filters. This result implies that, as expected, particles in the size classes $x > 1 \mu\text{m}$ are filtered. In conclusion, the measurement series with human aerosol sources show that the majority of the particles found in the classroom is in the size range of $x = 0.2\text{--}0.3 \mu\text{m}$ (lower end of the detectable size range of Fidas® Frog). This size is similar to the typical most penetrating particle size of many filters (Brown, 1993).

3.3.3. CO_2 - concentration vs. particle number concentration

In many publications, it is discussed that the CO_2 concentration in a room may also be used as an indication for the concentration of exhaled particles (Rudnick & Milton, 2003). Fig. 7 represents the evolution of the CO_2 concentration in the presence of 15 people in a classroom. Within 50 min, the CO_2 concentration (yellow) increases due to the breathing of the people, whereas the particle concentration (grey) fluctuates around a constant level of approximately $c = 150 \text{ particles}/\text{cm}^3$. During the ventilation phase, the particle measurement was restarted beginning at 88 min, so that no values of the PN concentration exist for the period between 50 min and 88 min. The ventilation has increased the PN concentration from $c = 150$ up to $175 \text{ particles}/\text{cm}^3$ due to interchange with ambient air.

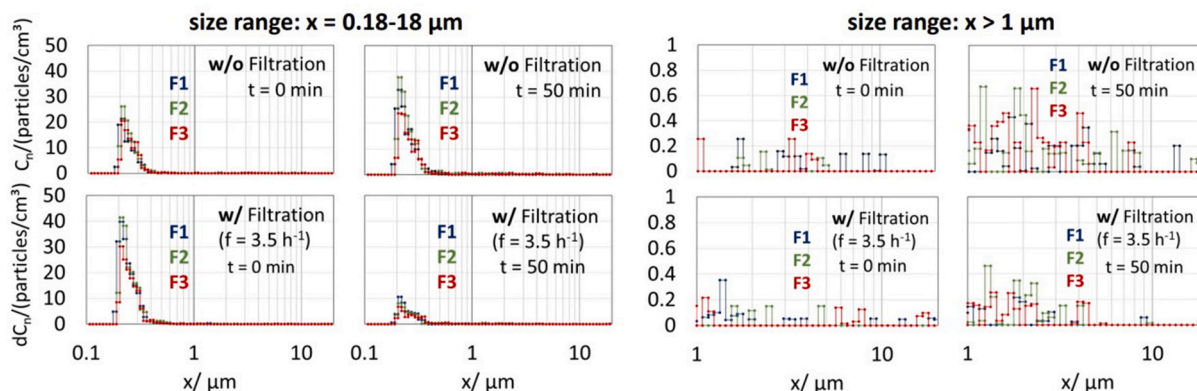


Fig. 6. Particle size distributions with & without filtration of the indoor air – human aerosol sources (For a better resolution different size ranges for the x & y -axis were chosen).

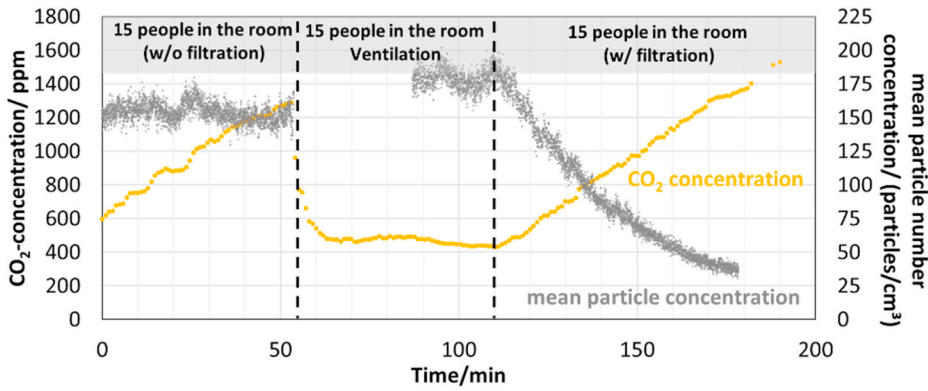


Fig. 7. Comparison of the CO₂-concentration and PN concentration.

The CO₂ concentration decreased within 10 min. Prolonged ventilation does not cause the CO₂ concentration to drop any further because the atmospheric concentration (410 ppm) was reached. Obviously, the indoor air has been efficiently replaced within 10 min. After stopping the ventilation phase and starting the mobile air filter, the CO₂ concentration in the air increases again due to people breathing in the room. The PN concentration in the room decreases due to filter operation. As the measurement shows, the PN concentration is dominated by the particle contributions of the ambient air, not representing a measure for the exhaled and possibly infectious particles. Therefore, no correlation between the number of particles and the CO₂ concentration could be derived. Since the virus concentration in infectious particles may vary, the PN concentration cannot be used to provide a clear indication of the risk of infection. The CO₂ sensors can be applied for qualitative monitoring of CO₂ concentration in rooms and as an indicator for the need for a ventilation phase.

3.3.3.1. *Scenario 3: temporal strong point source (concentration hotspot).* In this scenario, a temporarily present “superspreader” is simulated by investigating the influence of a strong point source on the PN concentration. The temporal and spatial evolution of particle concentration and size distribution was detected for two modes of filter operation. Therefore, two experiments were performed. First, the classroom was ventilated for 15 min. Subsequently, the aerosol source generated a particle aerosol at the singular position of the aerosol generator (AGK 2000) for 10 min. After particle generation, the natural dispersion of the aerosol in the room was examined in the first experiment. After ventilation, in the second experiment, the dispersion of the aerosol was recorded with simultaneous filtering of the indoor air by the mobile air filter I ($\dot{V} = 770 \text{ m}^3/\text{h}$). Here, the US-HEPA filter element was used (compare to scenario 2). For metrological reasons the number of particles generated by the artificial aerosol generator (approximately $c = 560,000 \text{ particles}/\text{cm}^3$) is set to be significantly higher than the number of particles actually emitted by a single infected person (Ma et al., 2020; Wei & Li, 2016).

Fig. 8 shows the temporal evolution of the PN concentration for the two experiments (with and without filter operation) during all three phases: Ventilation, particle generation, and decay. The PN concentration in the room was recorded continuously during the three phases in both measurements. However, for a better resolution of the particle dispersion, different time axes were selected. The PN concentration of the two measurements was related to the initial concentration c_0 of the measurement series with filtration. During the ventilation phase, the source is still switched off. In the case without filtration, the particle concentration increases at all three

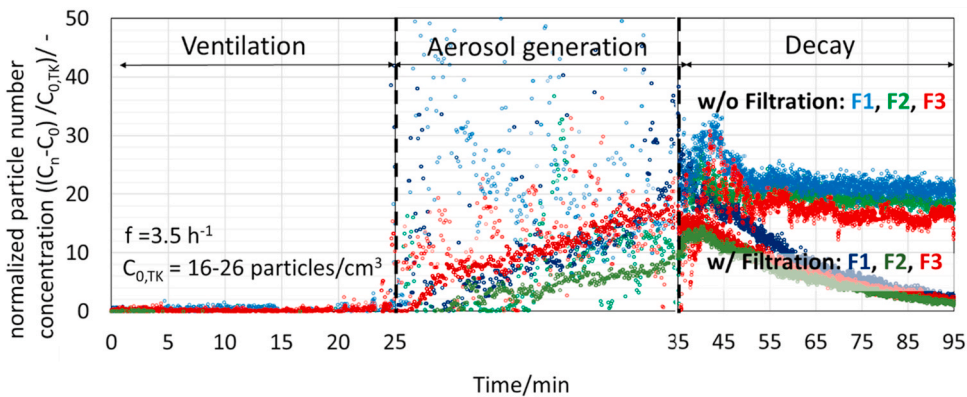


Fig. 8. PN concentration with & without filtration of the indoor air - strong point source (For a better resolution of the aerosol dispersion, different time axes were chosen).

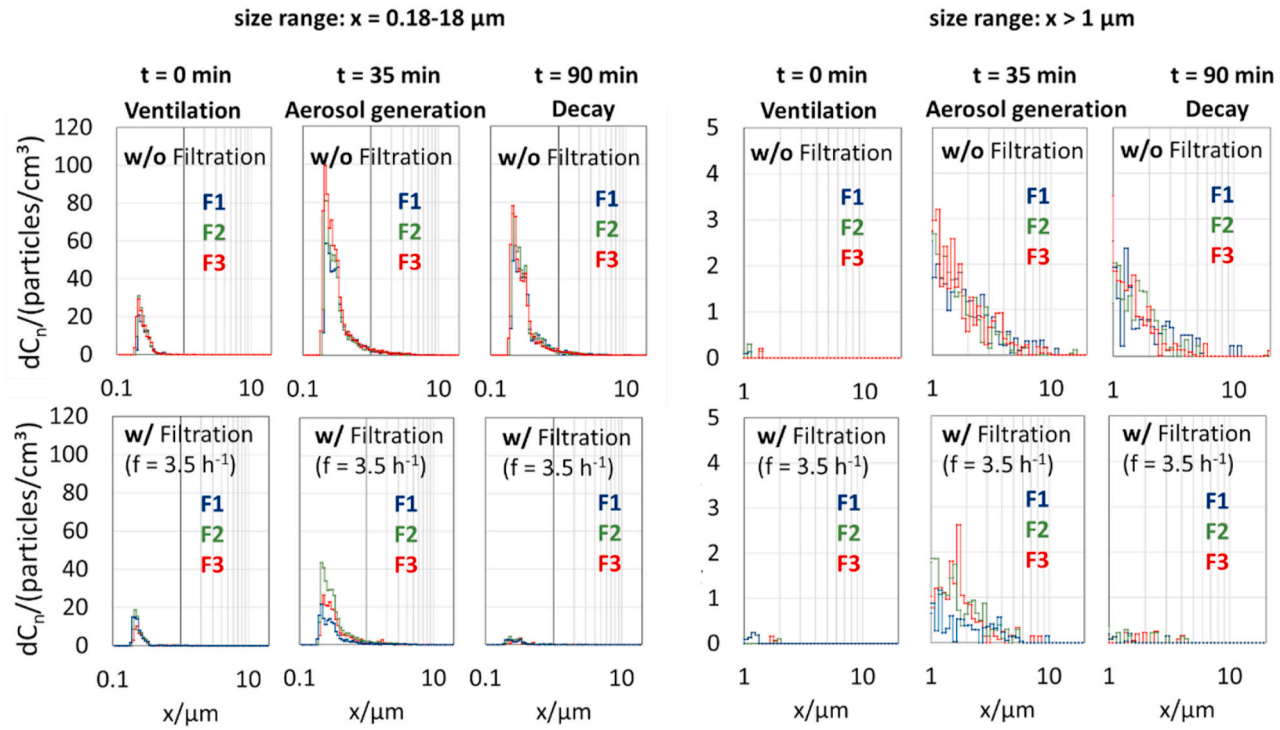


Fig. 9. Particle size distribution with & without filtration of the room air - strong point source (For a better resolution different size ranges for the x & y -axis were chosen).

positions after the ventilation phase due to aerosol generation within 10 min. The local PN concentration fluctuates strongly ($c = 320\text{--}1560$ particles/cm³). In particular, the measurement position near the aerosol generator outlet shows an increased particle concentration of $c = 960\text{--}1560$ particles/cm³ (light blue curve). After particle generation is stopped (last segment of Fig. 8), the particle concentration increases slightly because the particles in the room still have to spread out.

The particles disperse within approximately 10 min. In the experiment without filtration, the PN concentration remains at an almost constant level during the decay phase. This level is approximately twice as high as the maximum PN concentration at the end of the aerosol generation phase with filtration. In the experiment with filter operation, the PN concentration during ventilation $c_{0,TK}$ is approximately $c = 16\text{--}26$ particles/cm³. During aerosol generation, the particle concentration also increases at all three positions despite filtering. Compared to the experiment without filtration, streaking only occurs in the immediate vicinity of the aerosol source. The airflow created by the operation of the mobile air filter distributes the particles more evenly in the room, which limits the formation of streaks at F2 and F3. Thus, direct droplet transmission of infectious particles near a source cannot be completely prevented by filtration. After particle generation, the mobile air filter lowers the PN concentration almost to the initial concentration within 60 min. The comparison of the two-measurement series at 95 min further shows the effectiveness of the filter, due to the 10 times higher decrease in particle concentration as a result of filtration.

Fig. 9 displays the evolution of particle size distributions measured at the three positions (F1 – F3) with and without operation of the mobile air filter I at three different times. The diagrams on the right side of Fig. 9 show a section of the particle size spectrum from $x = 1\text{--}20$ μm to improve the visibility of the lower size-resolved concentrations. Mainly Particles $x < 1$ μm are introduced into the room through ventilation. Due to the simultaneous filtration during ventilation, the initial PN concentration is lower than the concentration resulting from ventilation without filtration. The active point source in the room mainly increases the PN concentration in the size classes $x < 1$ μm, as more particles are generated in the size fractions around $x = 0.3$ μm. At the time of aerosol generation ($t = 35$ min) (without filtration), the PN concentration in the size classes $x < 1$ μm has increased to a maximum of $c = 100$ particles/cm³. In comparison, particle generation (with filtration) only yields a maximum particle concentration of $c = 43$ particles/cm³ in the considered size classes $x < 1$ μm. About 60 min after switching off the aerosol source, a PN concentration of maximum $c = 4.38$ particles/cm³ in the size classes $x < 1$ μm is measured when the filter is operating. Without filtration, a maximum of $c = 80$ particles/cm³ is reached after 90 min. Consequently, the PN concentration in the size range of $x = 0.2\text{--}0.3$ μm is lowered by 90 % with filter operation whereas the natural decrease without filter operation is only 20 %.

Trends in particle separation of fractions $x > 1$ μm during ventilation are derived from Fig. 9. During the aerosol generation, a slightly lower PN concentration in the size classes $x > 1$ μm is observed with filter operation compared to without. Additionally, the overall number concentration of these size classes is very low and likely influenced by individual counting events. In case of filter operation for a long time without sources in the room, the PN concentration drops to almost zero for particles $x > 1$ μm. Therefore, the filter is effective in the entire size range of $x = 0.18\text{--}18$ μm.

3.3.4. Application: seminar room

The seminar room application demonstrates the impact of filter orientation and the airflow rate on the spatially and temporally resolved particle concentration evolution and shows the comparison with cross-flow ventilation. Since the volume flow range of the previous mobile air filter I was limited (see Table 3), the more powerful mobile air filter II was applied for measurements in the larger seminar room.

3.3.4.1. Scenario 1 + 4: Decay curves & impact of filter orientation. The seminar room is elongated and therefore deviates from the

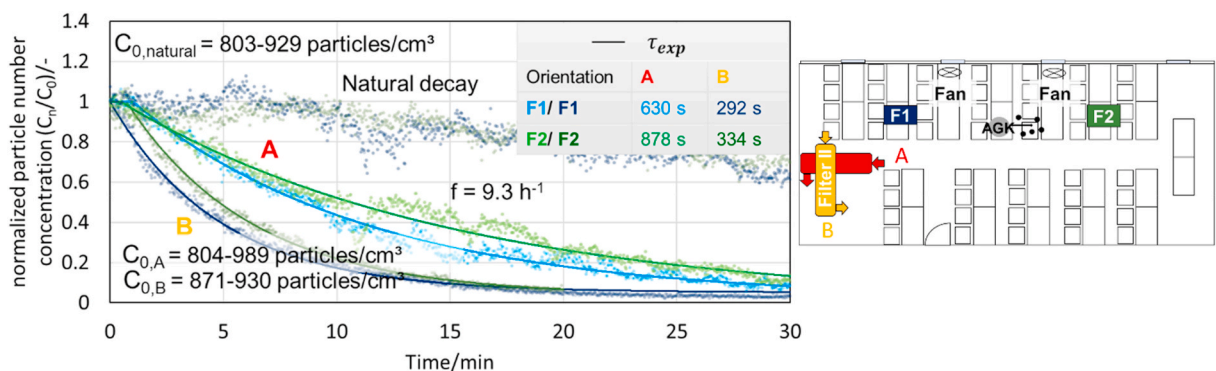


Fig. 10. Decay curves in the seminar room at orientation A & B of mobile air filter II – HEPA H14.

previous room geometries. Fig. 10 (right) shows the schematic floor plan of the room (268 m³) and the two orientations of the mobile air filter II. In orientation A of the mobile air filter, the air is drawn in from the front and discharged to the side. In orientation B, the air is drawn in from the side and discharged to the front. The aerosol source was in the center of the room. One particle measurement device was located near the mobile air filter (F1) and one at a greater distance from the mobile air filter (F2).

The procedure was identical for both orientations of mobile air filter II. First, the room was ventilated for 15 min. Then the aerosol generator was switched on for about 60 min, while the resulting particles were evenly distributed in the seminar room using additional fans. After the fans and the aerosol generator were switched off, the air in the room was filtered ($\dot{V} = 2500 \text{ m}^3/\text{h}$). In another experiment, the particle concentration decay due to cross-flow ventilation (instead of filtering) was measured after the aerosol generation.

Fig. 10 displays the simultaneously measured PN concentration at the two positions F1 and F2 for the two orientations of the mobile air filter II in the seminar room as well as the results of the calculation model including LS-approximations.

For orientation A of the mobile air filter, filtration and mixing occurs faster ($\tau_{\text{exp}}(\text{F1}) < \tau_{\text{exp}}(\text{F2})$) in the vicinity of the filter (F1), as the PN concentration decreases more rapidly than at position F2 further away from the filter. However, the difference in local residence time τ_{exp} at the two points F1 and F2 is relatively small (approximately 3 min). By changing the orientation of the mobile air filter II in the room (orientation B), the flow conditions in the investigated section in the room are significantly improved regarding effective filter operation, so that the local concentration decrease is even faster than the nominal average decrease ($\tau_{\text{exp}} < \tau_{\text{F}} = 387 \text{ s}$). The PN concentration also decreases faster near the filter (F1) than at a larger distance (F2), indicating potential short-circuit flows near the mobile air filter, and possible “dead zones” with reduced flow rates in sections of the room far away from the filter (and outside of the selected measurement positions F1 and F2). This is consistent with the statement by Kähler (Kähler et al., 2020b) who pointed out that a reduction of the wall jet occurs due to objects or with increasing distance due to wall friction, turbulent air movement, and entrainment. Turbulence primarily causes jet spreading, which locally reduces momentum and shifts the detachment position of the wall jet closer to the mobile air filter. As a result, the front region of an elongated room (close to the mobile air filter) is well filtered, while the rear region tends to be less filtered (Etheridge & Sandberg, 1996).

3.3.4.2. Scenario 4: comparison of filter operation vs. cross-flow ventilation. Fig. 11 shows the relative decrease in particle concentration due to cross-flow ventilation in comparison to the concentration decay due to filter operation (orientation B). The fitting parameters are summarized in Table 7. The temporal decrease was again recorded at the two positions F1 and F2. Cross-flow ventilation causes a

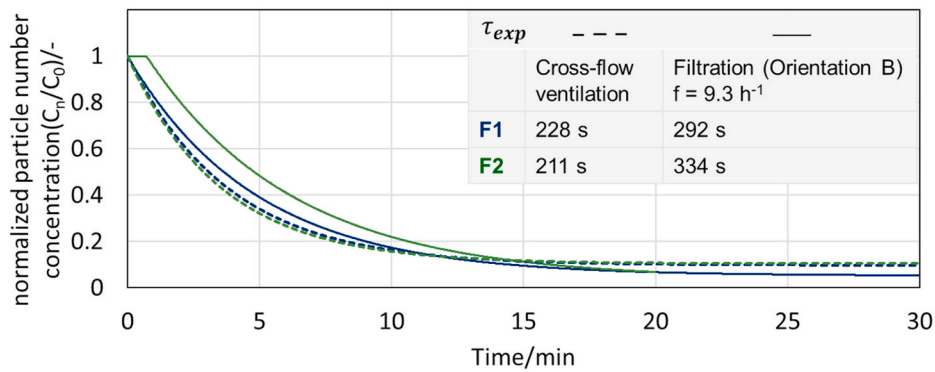


Fig. 11. Decay curves in the seminar room at orientation B of mobile air filter II - HEPA H14 and cross-flow-ventilation.

Table 7
LS-fitting parameters.

	Filtration - $f = 9.3 \text{ h}^{-1}$		Cross-flow ventilation	
	F1	F2	F1	F2
$C_0/(\#/ \text{cm}^3)$	871	930	659	548
$C_\infty/(\#/ \text{cm}^3)$	44	35	71	64
$\tau_{\text{exp}}/\text{s}$	292	334	228	211
t_{dead}/s	0	43	0	0

decrease in local PN concentrations at the two measuring positions F1 and F2 at similar rates for both positions. Based on the local residence times of the LS-approximation from Fig. 11, it can be shown that cross-flow ventilation in our case lowers the indoor particle concentration approximately 30 % faster than filtration with a filtration rate of 9.3 h^{-1} does. However, the resulting dilution of the indoor particle concentration by cross-flow ventilation strongly depends on the structural conditions (here: 4 windows with $A = 0.52 \text{ m}^2$ each, door size ($A = 2 \text{ m}^2$)) and the indoor and outdoor conditions such as temperature difference (here: $\Delta T \sim 10 \text{ K}$) between indoor and outdoor air or wind speeds. After approximately 15–20 min of filter operation, a steady-state concentration is achieved which is lower than the concentration achieved by cross-flow-ventilation only.

4. Summary and conclusion

Aerosol particles are currently considered to be the main transmission route for SarsCoV2 viruses. The mitigation of potentially infectious exhaled particles in the air is therefore of great importance in lowering the risk of infection. Mobile air filters represent a possibility to reduce the particle concentration in closed indoor environments.

In this paper, the effect of two different mobile air filters is investigated concerning their influence on the temporal development of the size- and spatially-resolved PN concentration in three application cases (office room, elementary school classroom, seminar room), for different filter specifications (US-HEPA, HEPA H14), operating conditions and orientations of the mobile air filters.

The spatial, temporally resolved development of the particle size distribution and concentration was determined with multiple identical mobile particle counters (Fidas Frog®, Palas®). The temporal development of the decrease in PN concentration in a closed indoor environment was described mathematically based on a simplified CSTR model. Experimental data and the fitting curves are in good agreement and smaller deviations between measurement and calculations are pointed out and discussed (differences between ideal and real indoor air mixing result in different fitting parameters for different scenarios).

Experiments performed in a small office room ($V = 103 \text{ m}^3$ – no people present), show that the use of a mobile air filter equipped with a highly effective filter medium (US-HEPA) and operated at a high volume flow rate ($f=9.2 \text{ h}^{-1}$) can very quickly reduce the particle concentration in the room air.

Experiments in an elementary school classroom occupied by 15 people during two consecutive regular school lessons (45 min each) initially showed that the people present during the experiment (13 of them not wearing masks) were no major particle sources. Despite the presence of people, the particle concentrations in the range of $c = 135\text{--}163 \text{ particles/cm}^3$ (depending on the measuring position) hardly changed during the first school lesson (without operating the filter). Due to the high level of background particles, no correlation could be found between the weak source of exhaled particles and the CO_2 concentration.

By operating a mobile air filter at a flow rate of $\dot{V} = 770 \text{ m}^3/\text{h}$ during the 2nd lesson ($f=3.5 \text{ h}^{-1}$), the PN concentration was continuously reduced during the school lesson, while the CO_2 concentration in the room air continuously increased - as in the first school lesson. The analysis of the spatio-temporal development of the particle size distributions showed that the investigated air filters effectively reduced the predominant submicron particles. Potentially virus-laden particles are in a size range of around 300 nm. Therefore, filter concepts need to ensure that these size classes are reduced at a high removal rate.

The temporary presence of a so-called “superspreader” in a classroom was simulated by a strong local aerosol point source (and no additional people in the room), which generated particles in the submicron size range with a high number concentration in the room for a certain time. When a mobile indoor air filter was operated, the increase in particle concentration was lower compared to the condition without the air filter during the period of aerosol generation. After switching off the strong particle source, the PN concentration also decreases continuously and uniformly. Despite the mobile air cleaner being switched on, high particle concentrations occur in the room air in the immediate vicinity of the aerosol source.

In the seminar room-application, the influence of the orientation of the filter device on the temporal and spatial development of the PN concentration was determined. It can be shown that the orientation of air intake and outlet of the filter device within the room - and thus, the overall set-up of the device - influences the temporal development of the PN concentration at two different positions in the room. Finally, the operation of the mobile air filter II with a high filtration rate was compared to the case of cross-ventilation of the room. It was shown that under certain conditions (very high filtration rate of 9.3 h^{-1}), the PN concentration in the investigated seminar room drops evenly within the room and almost as fast as in the case with cross-flow ventilation (by opening windows and the opposite door).

Funding sources

This work was financially supported by MANN + HUMMEL GmbH, Ludwigsburg. Through co-author Dr. Martin Lehmann, the sponsor was involved in the selection of suitable rooms for the measurements, in providing parts of the measurement equipment, in advising on the operational parameter settings of the mobile air filter, in assisting in the analysis of the measurement data and proofreading.

Declaration of competing interest

The authors declare that they have no known competing financial interests or personal relationships that could have appeared to influence the work reported in this paper.

Acknowledgments

We would like to thank MANN + HUMMEL for the financial support of the project. Thanks also go to Thomas Pemsel and Dr. Christoph Schulz for supporting the project. We would also like to thank the community school Eggenstein-Leopoldshafen for the possibility to perform experiments in their classroom and are grateful for the local helpfulness and support.

References

- Asadi, S., Wexler, A. S., Cappa, C. D., Barreda, S., Bouvier, N. M., & Ristenpart, W. D. (2019). Aerosol emission and superemission during human speech increase with voice loudness. *Scientific Reports*, 9(1), 2348.
- ASHRAE. (2021). *ASHRAE position Document on filtration and air cleaning*. Retrieved 11.10.21, from <https://www.ashrae.org/file%20library/about/position%20documents/filtration-and-air-cleaning-pd.pdf>.
- Bluyssen, P. M., Ortiz, M., & Zhang, D. (2021). The effect of a mobile HEPA filter system on 'infectious' aerosols, sound and air velocity in the SenseLab. *Building and Environment*, 188, 107475.
- Brown, R. C. (1993). *Air filtration: An integrated approach to the theory and applications of fibrous filters* (1. ed.). Oxford: Pergamon Press.
- Curtius, J., Granzin, M., & Schrod, J. (2021). Testing mobile air purifiers in a school classroom: Reducing the airborne transmission risk for SARS-CoV-2. *Aerosol Science and Technology*, 55(5), 586–599.
- Edwards, D. A., Man, J. C., Brand, P., Katstra, J. P., Sommerer, K., Stone, H. A., et al. (2004). Inhaling to mitigate exhaled bioaerosols. *Proceedings of the National Academy of Sciences of the United States of America*, 101(50), 17383–17388.
- Etheridge, D. W., & Sandberg, M. (1996). *Building ventilation: Theory and measurement*. Chichester: Wiley.
- Fabian, P., McDevitt, J., DeHaan, W., Fung, R., Cowling, B., Chan, K., et al. (2008). Influenza virus in human exhaled breath: An observational study. No. p. 2691 *PLoS One*.
- GAeF. (2020). *Positionspapier der Gesellschaft für Aerosolforschung: zum Verständnis der Rolle von Aerosolpartikeln beim SARS-CoV-2 Infektionsgeschehen*. Retrieved 6.8.21, from www.info.gaef.de.
- Hartmann, A., Lange, J., Rothardt, H., & Kriegel, M. (2020). *Emissionsrate und Partikelgröße von Bioaerosolen beim Atmen, Sprechen und Husten*.
- Haslbeck, K., Schwarz, K., Hohlfield, J., Seume, J., & Koch, W. (2010). *Submicron droplet formation in the human lung* (No. Bd. 41 pp. 429-438). *Journal of Aerosol Science*.
- Jayaweera, M., Perera, H., Gunawardana, B., & Manatunge, J. (2020). Transmission of COVID-19 virus by droplets and aerosols: A critical review on the unresolved dichotomy. *Environmental Research*, 188, 109819.
- Kähler, C. J., Fuchs, T., & Hain, R. (2020a). *Can mobile indoor air cleaners effectively reduce an indirect risk of SARS-CoV-2 infection by aerosols?*.
- Kähler, C. J., Fuchs, T., & Hain, R. (2020b). *Quantification of a Viromed Klinik Akut V 500 disinfection device to reduce the indirect risk of SARS-CoV-2 infection by aerosol particles*.
- Kähler, C. J., Fuchs, T., & Hain, R. (2021). *Qualification of the UniBw protection concept in different rooms of the Obermenzing high school*.
- Kähler, C. J., Fuchs, T., Mutsch, B., & Hain, R. (2020). *School education during the SARS-CoV-2 pandemic - which concept is safe, feasible and environmentally sound?*.
- Kähler, C. J., & Hain, R. (2020). Fundamental protective mechanisms of face masks against droplet infections. *Journal of Aerosol Science*, 148, 105617.
- Küpper, M., Asbach, C., Schneiderwind, U., Finger, H., Spiegelhoff, D., & Schumacher, S. (2019). Testing of an indoor air cleaner for particulate pollutants under realistic conditions in an office room. *Aerosol and Air Quality Research*, 19(8), 1655–1665.
- Lindsley, W., B, F., & Beezhold, D. e. a. (2016). *Viable influenza A virus in airborne particles expelled during coughs versus exhalations*. *Influenza and Other Respiratory Viruses*.
- Lu, J., Gu, J., Li, K., Xu, C., Su, W., Lai, Z., et al. (2020). COVID-19 outbreak associated with air conditioning in restaurant, guangzhou, China, 2020. *Emerging Infectious Diseases*, 26(7), 1628–1631.
- MANN+HUMMEL. (2020). from <https://www.mann-hummel.com/de/das-unternehmen/aktuelle-themen/pressemitteilungen/2020/lebensqualitaet-durch-antivirale-luftreiner-zurueckgewinnen/>.
- Ma, J., Qi, X., Chen, H., Li, X., Zhang, Z., Wang, H., et al. (2020). COVID-19 patients in earlier stages exhaled millions of SARS-CoV-2 per hour. *Clinical infectious diseases*. an official publication of the Infectious Diseases Society of America.
- Milton, D. K., Fabian, M. P., Cowling, B. J., Grantham, M. L., & McDevitt, J. J. (2013). Influenza virus aerosols in human exhaled breath: Particle size, culturability, and effect of surgical masks. *PLoS Pathogens*, 9(3), Article e1003205.
- Morawska, L., & Cao, J. (2020). Airborne transmission of SARS-CoV-2: The world should face the reality. *Environment International*, 139, 105730.
- Narayanan, S. R., & Yang, S. (2021). Airborne transmission of virus-laden aerosols inside a music classroom: Effects of portable purifiers and aerosol injection rates. *Physics of Fluids*, 33(3), 33307.
- Novoselac, A., & Siegel, J. A. (2009). Impact of placement of portable air cleaning devices in multizone residential environments. *Building and Environment*, 44(12), 2348–2356.
- Rudnick, S. N., & Milton, D. K. (2003). Risk of indoor airborne infection transmission estimated from carbon dioxide concentration. *Indoor Air No*, 13, 237–245.
- Scheuch, G. (2020). Breathing is enough: For the spread of influenza virus and SARS-CoV-2 by breathing only. *Journal of Aerosol Medicine and Pulmonary Drug Delivery*, 33(4), 230–234.
- Schumacher, S., Asbach, C., & Schmid, H.-J. (2021). Effektivität von Luftreinigern zur Reduzierung des COVID-19-Infektionsrisikos/Efficacy of air purifiers in reducing the risk of COVID-19 infections. *Gefahrstoffe*, 81, 16–28, 01-02.
- Schwarz, K. (2012). *Zur Entstehung, Charakterisierung und diagnostischen Nutzbarkeit in der menschlichen Lunge endogen generierter exhalierter Aerosole*. Zugl.: Clausthal, Techn. Univ., Diss. Univ.-Bibliothek Clausthal, 2012. Clausthal-Zellerfeld.
- Schwarz, K., Biller, H., Windt, H., Koch, W., & Hohlfield, J. M. (2010). Characterization of exhaled particles from the healthy human lung—a systematic analysis in relation to pulmonary function variables. *Journal of Aerosol Medicine and Pulmonary Drug Delivery*, 23(6), 371–379.
- Schwarz, K., Biller, H., Windt, H., Koch, W., & Hohlfield, J. M. (2015). Characterization of exhaled particles from the human lungs in airway obstruction. *Journal of Aerosol Medicine and Pulmonary Drug Delivery*, 28(1), 52–58.
- Wei, J., & Li, Y. (2016). Airborne spread of infectious agents in the indoor environment. *American Journal of Infection Control*, 44(9 Suppl), S102–S108.
- Zhang, R., Li, Y., Zhang, A. L., Wang, Y., & Molina, M. J. (2020). Identifying airborne transmission as the dominant route for the spread of COVID-19. *Proceedings of the National Academy of Sciences of the United States of America*, 117(26), 14857–14863.